THE UNIVERSITY OF MICHIGAN

COLLEGE OF ENGINEERING
Department of Aeronautical and Astronautical Engineering
High Altitude Engineering Laboratory

Technical Report

LONG-TERM INTEGRITY OF THE TIROS 5-CHANNEL RADIOMETER VISIBLE CHANNEL CHARACTERISTICS

F. L. Bartman
M. T. Surh
M. G. Whybra

ORA Project 03615

under contract with:

NATIONAL AERONAUTICS AND SPACE ADMINISTRATION
GODDARD SPACE FLIGHT CENTER
CONTRACT NO. NASw-140

administered through:

OFFICE OF RESEARCH ADMINISTRATION ANN ARBOR

December 1963

TABLE OF CONTENTS

UNIVERSITY OF MICHIGAN CALIBRATION PERSONNEL

F. L. Bartman, M.A., Research Engineer
L. W. Chaney, B.A., Research Engineer
V. B. Devlin, Assistant in Research
M. T. Surh, M.A., Assistant Research Engineer
M. G. Weimeister, Technician
M. G. Whybra, M.A., Associate Research Engineer
E. A. Work, Jr.,* B.S., Assistant Research Engineer

*Now at Bendix Systems Division, Ann Arbor, Michigan.

LIST OF TABLES

LIST OF FIGURES

ABSTRACT

The integrity of the visible channel calibrations of the TIROS 5-channel radiometer unit No. 103A is discussed. During a 16-month period, the radiometer experienced approximately 75 hours of near-space environment on balloon flights of 22-miles altitude and in environmental test chambers simulating conditions at 22 miles. Data from three sets of calibrations made during this time are shown to agree within the error of the measurements. The theory and method of making the calibrations are discussed.

1. INTRODUCTION

The meteorological satellites TIROS II, III, IV, and VII have each used a Barnes Engineering Company 5-channel Radiometer[1] for the measurement of the thermal radiation emitted by the earth and its atmosphere and of the solar radiation reflected and scattered by the same agents.[2] A radiometer of the same type has been used by The University of Michigan's High Altitude Engineering Laboratory for similar measurements on balloon flight tests at an altitude of approximately 115,000 feet.

One of the most important factors in the interpretation of the data measured by a radiometer is a knowledge of its operational characteristics, a thorough understanding of which is best obtained by frequent, careful calibrations. Ideally these calibrations would be made under the same environmental conditions experienced by the satellite-borne instrument. Also it is desirable to make calibrations both before and after flight data are obtained, so that possible changes in instrument characteristics can be detected.

The requirement of calibration under proper environmental conditions was certainly met in the preparation of the radiometers for the TIROS flights,[3] however, post-flight calibrations are impossible for the satellite work since the radiometer is not recovered.

The radiometer on the balloon flight tests can provide some knowledge of the integrity of the instrument characteristics after it has been used for some time under near-space conditions. The TIROS 5-channel radiometer No. 103A was flown on balloons four times between May 1961 and September 1962. In addition, the radiometer was operated under simulated balloon-flight environmental conditions four times during this period. The total time of operation under near-space conditions during this period approximates 75 hours. Calibrations were made in May 1961, in August 1961, and in September 1962 at the NASA Goddard Space Flight Center; additional calibrations were made at The University of Michigan.

The purpose of this report is to discuss a portion of these calibration data to see what they reveal about the long-term integrity of the characteristics of the visible channels of this radiometer. Future reports will consider the visible channel calibrations at Michigan, the thermal channel calibrations at NASA and Michigan, and will attempt to establish the absolute accuracy of all of these calibrations.

2. DESCRIPTION OF THE RADIOMETER

The principle of the TIROS 5-channel radiometer is illustrated schematically in Fig. 1, showing the basic components of a single channel of the radiometer. The field of view of each channel is about 5° wide at the half power-point (the field of view down to 5% of maximum response is 8 to 9°). The chopper disk-prism arrangement causes the radiometer to look alternately in opposite directions. During flight and during calibration, a reference target is viewed in one direction, and the earth or calibration target in the opposite direction. The reference target is outer space during flight and is a liquid nitrogen-cooled black body during calibration. As the half mirror-half black chopper disk rotates, the radiation reaches the detector alternately from opposite directions. The resulting chopped signal is amplified and rectified to produce a D.C. signal, which in the ideal instrument is proportional to the difference in energy flux received from the two directions. The two viewing directions are called "wall" and "floor" side of the radiometer according to their location in the TIROS satellite, i.e., one view is through the wall side, the other through the floor side of the satellite.

The nominal characteristics of the two visible channels, channels 3 and 5, with whose calibration we are concerned in this report, are given in Table I.

TABLE I

NOMINAL CHARACTERISTICS OF TIROS RADIOMETER

CHANNEL 3 AND CHANNEL 5

Channel Number	3	5
Purpose of Measurement	"Reflected" Solar Radiation	Comparison with TV-Photos
Wave-length (Nominal)	.2-6 microns	.55-.75 microns
Optics (lenses)	Al_2O_3 BoF_2	Al_2O_3 SiO_2
Filters	----	Interference and Chance Glass

3. METHOD OF CALIBRATION

The method of calibration used in the NASA calibrations of the visible channels of the TIROS 5-channel radiometer is referred to in the literature as the "Near-Extended Source Method."[4] A diffuse* source, larger than the radiometer aperture, which will completely fill the radiometer field of view, is placed within a short distance of the aperture so that the transmissivity of the medium between the source and the atmosphere is essentially unity. The equations which apply can be written as follows.

Assuming that:

a. The source is an ideal diffuse source of known spectral radiance $N_{\lambda c}$.

b. The transmissivity of the medium between the source and radiometer is unity.

The characteristics of the calibration source are given by

$$N_c = \int_0^\infty N_{\lambda c} d\lambda \qquad \text{watts-cm}^{-2}\text{-steradian}^{-1} \tag{1a}$$

$$W_c = \int_0^\infty W_{\lambda c} d\lambda \qquad \text{watts-cm}^{-2} \tag{1b}$$

and the relations

$$N_c = \frac{W_c}{\pi} \tag{2a}$$

$$N_{\lambda_c} = \frac{W_{\lambda c}}{\pi} \tag{2b}$$

Where:

$N_{\lambda c}$ is the spectral radiance, watts-cm^{-2}-steradian^{-1}-micron^{-1}

$W_{\lambda c}$ is the spectral radiant emittance, watts-cm^{-2}-micron^{-1}

N_c is the radiance, watts-cm^{-2}-steradian^{-1}

W_c is the radiant emittance, watts-cm^{-2}

*Diffuse in the sense of a Lambert radiator!

The irradiance of the radiometer aperture is

$$H_c = \Omega \cdot \int_0^\infty N_{\lambda c} d\lambda \qquad \text{watts-cm}^{-2} \qquad (3)$$

where Ω is the solid angle viewed by the radiometer. The total radiant power at the radiometer aperture is

$$H_c A_r = A_r \cdot \Omega \cdot \int_0^\infty N_{\lambda c} d\lambda \qquad \text{watts} \qquad (4)$$

where A_r is the effective area of the radiometer aperture.

If the response of the radiometer is constant over its entire field of view, the voltage output of the radiometer is given by

$$V_c = R \cdot A_r \cdot \Omega \cdot \int_0^\infty N_{\lambda c} \cdot \phi_\lambda d\lambda \qquad \text{volts} \qquad (5)$$

where R is the responsivity constant of the detector in volts$\cdot$watt^{-1}, and ϕ_λ is a quantity called the effective spectral response of the instrument, with maximum value ≤ 1, which accounts for the spectral response of the detector, the transmission of optical components such as filters and lenses, and the reflectivity of mirrors. We can write the last equation as

$$V_c = R \cdot A_r \cdot \Omega \cdot N_c' \qquad \text{(volts)} \qquad (6)$$

where

$$N_c' = \int_0^\infty N_{\lambda c} \phi_\lambda \cdot d\lambda \qquad \begin{matrix}\text{watts-cm}^{-2}\text{-} \\ \text{Steradian}^{-1}\end{matrix} \qquad (7)$$

is said to be the "effective" radiance of the source, i.e., the radiance of the source modified by the spectral response characteristics of the instrument.

In the practical case in which the response of the radiometer is not uniform over the entire field of view, we can write the voltage output of the radiometer as

$$V_c = A_r \cdot N_c' \int_\Omega R(\omega) \cdot d\omega \qquad (8)$$

where $R(\omega)$ is the responsivity of the radiometer as a function of the solid angle ω. Even in this case we can write

$$V_c = R' \cdot A_r \cdot \Omega \cdot N'_c \tag{9}$$

where R' is the responsivity of the detector averaged over the entire field of view, i.e.,

$$R' = \frac{\int_\Omega R(\omega) d\omega}{\Omega} \tag{10}$$

Thus the equation which describes the voltage output of the radiometer is (9) above, or, for this "diffuse" calibrating source,

$$V_c = R' \cdot A_r \cdot \Omega \cdot \frac{W'_c}{\pi} \tag{11}$$

Where W'_c is the "effective" radiant emittance of the diffuse source, i.e., the spectral radiant emittance of the source modified by the spectral response characteristics of the instrument, i.e.,

$$W'_c = \int_0^\infty W_{\lambda c} \phi_\lambda d\lambda \tag{12}$$

The calibration procedure for the visible channels of the radiometer unit No. 103A consisted of the following steps:

a. Vary $W_c = \int_0^\infty W_{\lambda c} d\lambda$ of the diffuse source of known spectral distribution.

b. Record corresponding values of V_c and W_c.

c. For a given value of W_c, calculate a corresponding value of W'_c. This can be done using Eq. (12) above if $W_{\lambda c}$ and ϕ_λ are known for the diffuse calibrating source and the radiometer respectively.

d. Plot curves of V_c vs. W_c, or V_c vs. W'_c (the latter is used in this report).

These curves are the "calibration curves" of the radiometer for a diffuse target of the given spectral radiant emittance. Since the calibration curves of the radiometer are not completely independent of the temperature of the

radiometer itself, there is a set of such calibration curves covering the range of temperatures over which the instrument is expected to operate, see Fig. 2.

The calibration at room temperature was made with a "standard" lamp as a source and is the absolute calibration. The possible changes of the calibration with radiometer temperature was investigated with another lamp, and only relative values were obtained.

Ideally, the instrument calibrated as indicated in this section would be used only with diffusely radiating unknown targets of the same spectral radiant emittance $W_{\lambda c}$ as the calibrating source, in which case the use of the calibration curves is quite straightforward. The interpretation of the data in the case in which the target is not diffuse or does not have the spectral distribution of the calibrating source is more difficult and will not be discussed further here.

The usefulness of the instrument depends on the calibration curves remaining constant over long periods. This stability is the subject of the reported investigation.

4. THE EFFECTIVE SPECTRAL RESPONSE

The effective spectral response of a channel of the radiometer is given by:[3]

$$\phi_\lambda = R_\lambda^p (R_\lambda^m - R_\lambda^b) \cdot f_\lambda \cdot A_\lambda \qquad (13)$$

where

R_λ^p is the spectral reflectivity of the radiometer prism

R_λ^m is the spectral reflectivity of the aluminized half of the chopper disk

R_λ^b is the spectral reflectivity of the black half of the chopper disk

f_λ is the spectral transmissivity of the filter-lens portion of the given channel

A_λ is the spectral absorptivity of the thermister detector.

In the actual computation of ϕ_λ, the expression

$$\phi_\lambda = R_\lambda^P (1 - R_\lambda^B) \cdot f_\lambda \qquad (14)$$

was used, thus assuming that $R_\lambda^M = 1$ and $A_\lambda = 1$. The data used to compute ϕ_λ for the visible channels of the radiometer are given in Section 7.

5. THE RADIANT EMITTANCE OF THE SOURCE

Figure 3 is a schematic diagram of the calibration arrangement. The diffuse calibration source was produced by reflection of light from white Kodak paper. The source of light was a type G.E. 30A/T24/3 lamp No. 6271, calibrated by the National Bureau of Standards and at the Naval Research Laboratories.

The apparatus consisted of a calibration rack containing fixed mounts for the standard lamp and the radiometer. Two white Kodak paper targets (of fixed radii of curvature 42.0 cm and 90.0 cm) could be placed at various distances from the lamp in order to vary the intensity of light reflected to the radiometer. The target of 42 cm radius of curvature was used at distances of 45.7, 48.2, 50.7, 53.2 and 55.7 cm from the lamp; the 90.0 cm radius of curvature target was used at 55.7, 57.7, 62.7, 72.7, 82.7, 92.7 and 102.7 cm from the lamp.

During the calibration measurements the standard lamp was operated at 15.30 amperes and 94.60 volts (RMS). The voltage was measured during the calibration with an NLS digital voltmeter with A.C. converter. Voltage fluctuations of approximately 0.5% were observed. The radiometer output voltage was measured with a Hewlett-Packard 410-B voltmeter.

Calibration data supplied by NASA personnel for the standard lamp consisted of:

a. The Bureau of Standards data; i.e., the luminous intensity of the lamp is 3455 candles under the above operating conditions.

b. A curve of relative spectral radiance ψ_λ (in arbitrary units) obtained by Naval Research Laboratory personnel (see Fig. 4) for the same operating voltage.

From this data the spectral radiant intensity of the source, can be calculated as follows. The luminous intensity of the lamp is given by

$$I = 685\ k \int_0^\infty \psi_\lambda k_\lambda d\lambda = 3455 \text{ candles} \qquad (15)$$

where

I is the luminous intensity in candles (lumens-steradians^{-1})

λ is the wavelength, in microns

685 is the luminous efficiency of monochromatic flux of wavelength 0.555 microns (lumens-watt^{-1})

ψ_λ is the relative spectral radiance, in arbitrary units

k_λ is the relative luminosity of a standard observer for good lighting conditions (see Fig. 5), i.e., the luminous efficiency at wavelength λ is 685 k_λ lumens/watt

k is a constant

Thus if we solve for k from Eq. (15), we find

$$k = \frac{3455}{685 \int_0^\infty \psi_\lambda k_\lambda d\lambda} \tag{16}$$

and the spectral radiant intensity of the NBS standard lamp is

$$J_\lambda = k\psi_\lambda \qquad \text{watts-steradian}^{-1}\text{-micron}^{-1} \tag{17}$$

The value of k obtained for the standard lamp No. 6271 obtained in this fashion is 39.084.

Since $J_{\lambda\ max}$ for the spectral radiant intensity of the NBS standard lamp occurs at a wavelength λ_{max} of 0.91 micron, the spectral distribution of the lamp is approximately that of 3170°K black body (see Fig. 4 for comparison).

The Kodak white paper is curved and the lamp located so that the radiation from the lamp is very nearly normally incident upon the paper. Under these conditions, the spectral radiant emittance of the calibration source (the Kodak paper) is

$$W_{\lambda c} = \frac{J_\lambda \cdot r_\lambda}{R^2} \qquad \text{watts-meter}^{-2}\text{-micron} \tag{18}$$

Where r_λ is the diffuse reflectivity of the white Kodak paper (Fig. 6) and R is the distance (in meters) from the standard lamp to the white paper.

The radiant emittance of the calibrating source is therefore

$$W_c = \int_0^\infty \frac{J_\lambda \cdot r_\lambda}{R^2} d\lambda \qquad \text{watts-meter}^{-2} \tag{19}$$

$$= k \int_0^\infty \frac{\psi_\lambda r_\lambda}{R^2} \qquad \text{watts-meter}^{-2} \tag{20}$$

6. THE "EFFECTIVE" RADIANT EMITTANCE OF THE SOURCE

The "Effective" radiant emittance of the calibration source was given by Eq. (12) above, i.e.,

$$W'_c = \int_0^\infty W_{\lambda c}\phi_\lambda d\lambda \qquad \text{watts-meter}^{-2}$$

where $W_{\lambda c}$ and ϕ_λ are given by Eq. (18) and (14) above, respectively.

The integration was performed numerically, by summing the contributions to the integral from each small increment of wavelength $\Delta\lambda_i$, thus

$$\begin{aligned} W'_c &= \sum_i (W_c)_i \phi_i \Delta\lambda_i \\ &= \frac{k}{R^2} \sum_i \psi_i r_i \phi_i \Delta\lambda_i \qquad \text{watts-meter}^{-2} \end{aligned} \qquad (21)$$

7. RESULTS

The data used to specify the calibration characteristics of the TIROS 5-channel radiometer No. 103A are given in Table II for channel 3, and in Table III for channel 5. ψ_r and r_λ are plotted in Figs. 4 and 6, as noted above. ϕ_λ and the product $k\psi_\lambda r_\lambda \phi_\lambda$ (the "effective" spectral radiant emittance of the Kodak white paper source) are given in Figs. 7 and 8 respectively for both channels.

The summation indicated in Eq. (21) was carried out, and the "effective" radiant emittance of the calibration source was found to be

$$\text{(Channel 3)} \qquad W_c' = \frac{66.74}{R^2} \quad \text{watts per meter}^2 \tag{22}$$

$$\text{(Channel 5)} \qquad W_c' = \frac{4.65}{R^2} \quad \text{watts per meter}^2 \tag{23}$$

The calibration data, i.e., values of V_c versus W_c' for 14 values of R taken with the radiometer at room temperature are given in Table IV for channel 3, and in Table V for channel 5. Complete sets of data were taken in May and August of 1961, and spot checks were made in September 1962.

Radiometer temperatures during the three calibration runs are shown in Table VI.

Figure 9 shows the temperature dependence of the calibration data (relative calibration curves) for channel 3, wall side; for convenience, a portion of the data is re-plotted in Fig. 10. Similarly, the temperature dependence of the calibration curves for channel 5, wall side, is shown in Fig. 11, with a portion of the data re-plotted in Fig. 12.

The data of May 1961 have been corrected to the radiometer temperature of the August 1961 and September 1962 data. For channel 3 the data were corrected to the radiometer temperature of 30°C. For channel 5 the data were corrected to the radiometer temperature of 31°C. The corrected calibration results are shown in Tables VII and VIII respectively, and are plotted in Figs. 13 and 14 respectively.

The May 1961 and August 1961 calibrations agree within the accuracy of the measurements. The September 1962 data show somewhat more scatter but are also essentially in agreement.

TABLE II

CHANNEL 3 CALIBRATION CHARACTERISTIC DATA

λ	f_λ	$1-R_\lambda^B$	R_λ^P	ϕ_λ	r_λ	$k\psi_\lambda$	$k\psi_\lambda\phi_\lambda r_\lambda$
Wavelength Microns	Filter-lens Transmissivity	Chopper Reflectivity	Prism Reflectivity	Effective Spectral Response	White Paper Reflectivity	Lamp Spectral Radiant Intensity	White Paper Effective Spectral Radiant Emittance
.25	.5155	.240	.619	.077	.60	---	---
.26	.6704	.371	.619	.154	.60	---	---
.28	.7592	.642	.636	.310	.63	---	---
.31	.7799	.788	.756	.465	.66	---	---
.41	.7887	.788	.870	.541	.78	5.081	2.144
.51	.7980	.852	.870	.592	.88	24.232	12.601
.61	.7999	.836	.800	.535	.88	77.386	36.449
.71	.8021	.795	.778	.496	.88	113.344	49.531
.81	.8026	.730	.750	.439	.897	127.414	50.201
.91	.8083	.750	.768	.466	.90	132.104	55.352
1.01	.8085	.782	.800	.506	.89	126.241	56.808
1.21	.8133	.812	.834	.551	.88	106.699	51.749
1.41	.8135	.830	.851	.575	.83	85.203	40.642
1.61	.8183	.850	.868	.604	.70	66.052	27.94
1.81	.8239	.860	.877	.621	.75	49.637	23.131
1.91	.8231	.870	.886	.634	.71	50.028	22.513
2.01	.8233	.875	.875	.630	.66	41.82	17.397
2.21	.8225	.890	.890	.652	.60	32.831	12.837
2.41	.8188	.905	.905	.671	.49	30.876	10.158
2.61	.8329	.86	.860	.616	.46	23.45	6.636
2.81	.8238	.86	.86	.609	.39	9.38	2.232
3.02	.8240	.87	.87	.624	.32	---	---
3.50	.8420	.88	.88	.652	---	---	---
4.10	.8259	.89	.89	.654	---	---	---
4.22	.8261	.90	.90	.669	---	---	---
4.34	.8214	.90	.90	.665	---	---	---
4.46	.7984	.89	.89	.632	---	---	---
4.58	.7789	.89	.89	.617	---	---	---

TABLE III

CHANNEL 5 CALIBRATION CHARACTERISTIC DATA

λ	f_λ	$1-R_\lambda^B$	R_λ^P	ϕ_λ	r_λ	$k\psi_\lambda$	$k\psi_\lambda\phi_\lambda r_\lambda$
Wavelength Microns	Filter-lens Transmissivity	Chopper Reflectivity	Prism Reflectivity	Effective Spectral Response	White Paper Reflectivity	Lamp Spectral Radiant Intensity	White Paper Effective Spectral Radiant Emittance
.500	.005	.854	.860	.0037	.88	21.494	.0633
.525	.060	.856	.845	.043	.88	29.455	1.099
.550	.241	.854	.830	.171	.88	41.794	6.156
.575	.459	.850	.814	.318	.88	55.726	15.321
.600	.332	.842	.798	.223	.88	71.647	13.789
.625	.350	.833	.782	.228	.88	85.977	16.969
.650	.342	.828	.767	.217	.88	98.714	18.512
.675	.358	.815	.748	.218	.88	107.471	20.261
.700	.250	.805	.732	.147	.88	113.441	14.481
.725	.245	.799	.887	.174	.887	117.82	17.816
.750	.137	.783	.892	.096	.892	122.198	10.199
.775	.010	.767	.895	.0069	.895	125.781	.741
.800	.000	.752	---	---	---	---	---
.							
.							
.							
1.10	.003	.819	.89	.0022	.89	121.402	.238
1.13	.016	.824	.89	.012	.89	117.82	1.167
1.20	.008	.832	.88	.0059	.88	109.859	.539
1.40	.013	.852	.84	.0093	.84	87.967	.691
1.60	.037	.862	.69	.0220	.69	68.065	1.003
1.80	.062	.876	.75	.041	.75	50.153	1.477
2.00	.062	.840	.84	.044	.67	43.386	1.236
2.20	.060	.850	.85	.043	.60	33.037	.843
2.40	.066	.860	.860	.049	.50	31.445	.741
2.60	.074	.868	.868	.056	.46	24.678	.630
2.70	.079	.870	.875	.060	.43	17.514	.447
2.80	.006	.865	.865	.0045	.39	9.951	.0195
2.90	.000	.870	.865	---	.36	2.786	---

TABLE IV

CALIBRATION RESULTS FOR CHANNEL 3

(Uncorrected for Temperature Dependence)

W'_c (watt-m^{-2})	Floor Side			Wall Side		
	May 1961	Aug. 1961	Sept. 1962	May 1961	Aug. 1961	Sept. 1962
	Volts			Volts		
319.6	6.02	5.86	5.94	5.58	5.08	5.16
287.3	5.46	5.46	--	5.04	4.52	--
259.7	4.98	4.90	--	4.54	4.24	4.24
235.8	4.54	4.44	--	4.20	3.96	--
215.2	4.18	4.16	4.00	3.78	3.68	3.64
219.0	4.28	4.14	--	3.82	3.66	3.44
200.5	3.92	3.82	--	3.56	3.28	3.18
169.8	3.38	3.26	--	3.18	2.90	--
145.6	2.88	2.84	2.64	2.74	2.46	2.32
126.3	2.54	2.46	--	2.42	2.12	--
110.6	2.28	2.18	--	2.12	1.88	1.78
97.6	1.86	1.82	--	1.74	1.62	--
77.7	1.62	1.58	1.44	1.46	1.33	1.32
63.3	1.32	1.25	--	1.20	1.10	--

TABLE V

CALIBRATION RESULTS FOR CHANNEL 5

(Uncorrected for Temperature Dependence)

W'_c (watt-m^{-2})	Floor Side			Wall Side		
	May 1961	Aug. 1961	Sept. 1962	May 1961	Aug. 1961	Sept. 1962
	Volts			Volts		
22.3	2.90	2.60	2.90	2.94	2.64	2.78
20.0	2.64	2.36	--	2.64	2.38	--
18.1	2.34	2.14	--	2.42	2.14	2.36
16.4	2.16	1.90	--	2.20	1.92	--
15.0	2.00	1.72	1.96	2.00	1.72	1.94-1.98
15.3	1.98	1.76	--	2.10	1.78	--
14.0	1.84	1.60	--	1.94	1.72	1.74
11.8	1.56	1.38	--	1.64	1.44	--
10.1	1.36	1.20	1.20	1.40	1.20	1.26
8.8	1.18	1.06	--	1.22	1.08	--
7.7	1.04	.90	--	1.10	.92	.98
6.8	.86	.76	--	.90	.76	--
5.4	.70	.62	.68	.74	.64	.64
4.4	.58	.52	--	.60	.52	--

TABLE VI

RADIOMETER TEMPERATURES DURING CALIBRATION RUNS

Date	Channel 3				Channel 5			
	Wall Side		Floor Side		Wall Side		Floor Side	
	Begin, °C	End, °C	Begin, °C	End, °C	Begin, °C	End, °C	Begin, °C	End, °C
May, 1961	25.8	27.5	28.5	29.0	28.4	27.6	29.3	29.2
Aug., 1961	29.8	30.5	31.1	31.0	30.7	31.1	31.0	31.1
Sept., 1962	29.1	29.9	30.6	30.6	30.0	30.2	30.6	30.6

TABLE VII

CALIBRATION RESULTS FOR CHANNEL 3 AT 30°C

(Corrected for the Radiometer Temperature)

W'_c (watt-m^{-2})	Wall Side		
	May, 1961	Aug., 1961	Sept., 1962
	Volts		
319.6	5.30	5.08	5.16
287.3	4.79	4.52	--
259.7	4.31	4.24	4.24
235.8	3.99	3.96	--
215.2	3.59	3.68	3.64
219.0	3.63	3.66	3.44
200.5	3.38	3.28	3.18
169.8	3.02	2.90	--
145.6	2.60	2.46	2.32
126.3	2.30	2.12	--
110.6	2.01	1.88	1.78
97.6	1.65	1.62	--
77.7	1.39	1.33	1.32
63.3	1.14	1.10	--

TABLE VIII

CALIBRATION RESULTS FOR CHANNEL 5 AT 30°C

(Corrected for the Radiometer Temperature)

W'_c (watt-m^{-2})	Wall Side		
	May, 1961	Aug., 1961	Sept., 1962
	Volts		
22.3	2.72	2.64	2.78
20.0	2.44	2.38	--
18.1	2.24	2.14	2.36
16.4	2.04	1.92	--
15.0	1.85	1.72	1.96
15.3	[illegible]	1.78	--
14.0	1.80	1.72	1.74
11.8	1.52	1.44	--
10.1	1.30	1.20	1.26
8.8	1.13	1.08	--
7.7	1.02	.92	.98
6.8	.83	.76	--
5.4	.68	.64	.64
4.4	.55	.52	--

8. DISCUSSION AND CONCLUSION

The accuracy of this evaluation of the long-term integrity of the channel 3 and channel 5 calibrations of the TIROS 5-channel radiometer depends on the ability to repeat and measure precisely the calibration source characteristics, the radiometer operating characteristics and the radiometer output voltage.

The factors which affect the repeatability of the calibration source characteristics are the stability of the light output of the lamp, the stability of the reflectivity characteristics of the Kodak white paper, the repeatability of the lamp to white paper distances and the lamp operating voltage.

The lamp is operated at about 85% of its normal operating voltage and thus should have a lifetime (500 hours ?) much longer than the time it was actually used. Although it is assumed that the lamp characteristics at the given voltage did not change during the 16 month interval over which the calibrations were carried out, it is felt that this assumption has not been checked well enough and that further use of this calibration apparatus would warrant additional calibrations of the characteristics of the lamp itself.

The reflectivity of the Kodak white paper can vary somewhat depending on the nature of the accumulation of surface dust. Similar reflecting surfaces of magnesium oxide show a 2% decrease in reflectivity after a short time of use, followed by a rather long period of stable reflectivity characteristics. We assume the same behavior for the Kodak white paper target and thus assume a maximum uncertainty of 2% in reflectivity characteristics.

The lamp voltage and lamp to white paper distance are repeatable within ± 0.5% and so contribute only a small uncertainty to the results.

The radiometer operating characteristics should repeat if all radiometer power supply voltages are kept at their proper values. Precautions are taken to monitor these voltages at intervals before and during the calibration runs and critical voltages are regulated.

The radiometer output voltage is read with a maximum error of ± 3% of full scale.

Table IX summarizes the estimates of the uncertainty which these various factors contribute to the calibrations. If these possible sources of error combine randomly, the net uncertainty would be ± 4%.

TABLE IX

UNCERTAINTY OF THE CALIBRATION DATA

Possible Source of Error	Uncertainty
Lamp Characteristics	---
Lamp Voltage	± 0.5%
White Paper Reflectivity	± 2.0%
Lamp to White Paper Distance	± 0.5%
Radiometer Operating Voltages	---
Radiometer Output Voltage	± 3%

The data in Figs. 13 and 14 are seen to have scattered less than this amount and so it must be concluded that, under laboratory conditions the calibrations of channel 3 and channel 5 of the TIROS 5-channel radiometer maintained their integrity over this 16 month interval within the limits of the uncertainty in the measurements (± 4%).

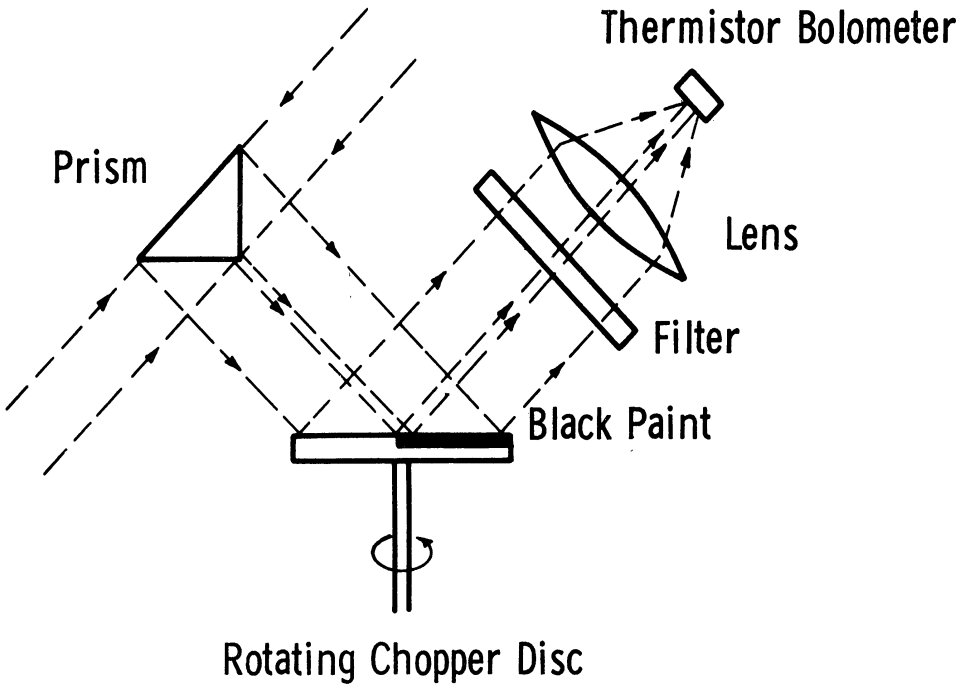

Fig. 1. Diagram indicating principle of operation of a channel of the TIROS 5-channel radiometer.

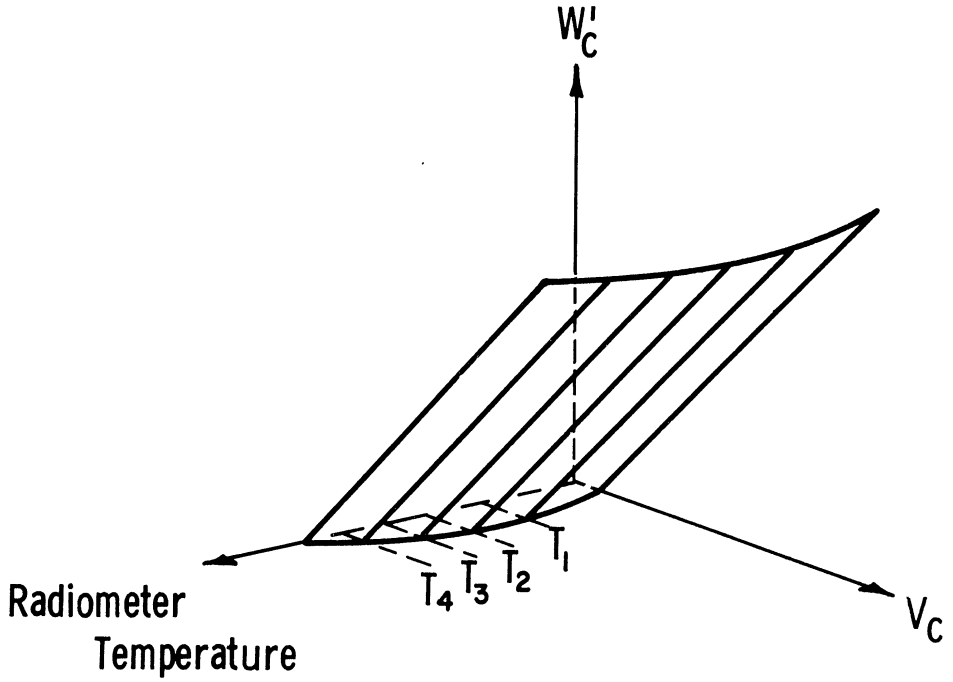

Fig. 2. Set of calibration curves obtained at several radiometer temperatures.

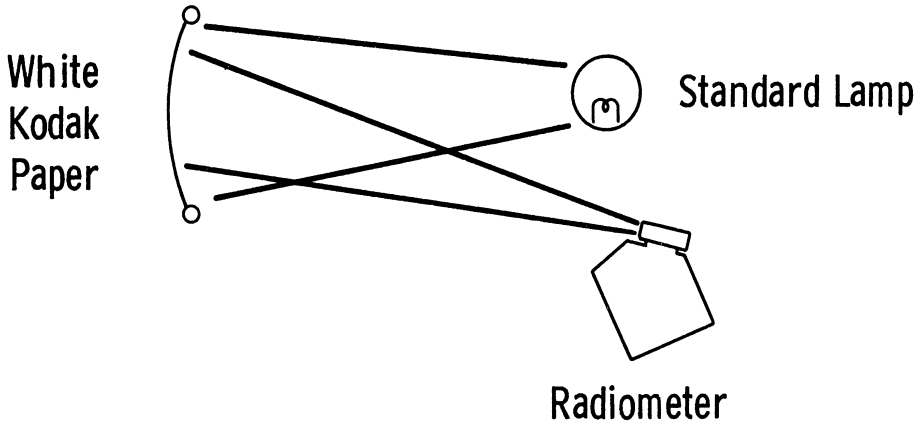

Fig. 3. Schematic diagram of calibration arrangement.

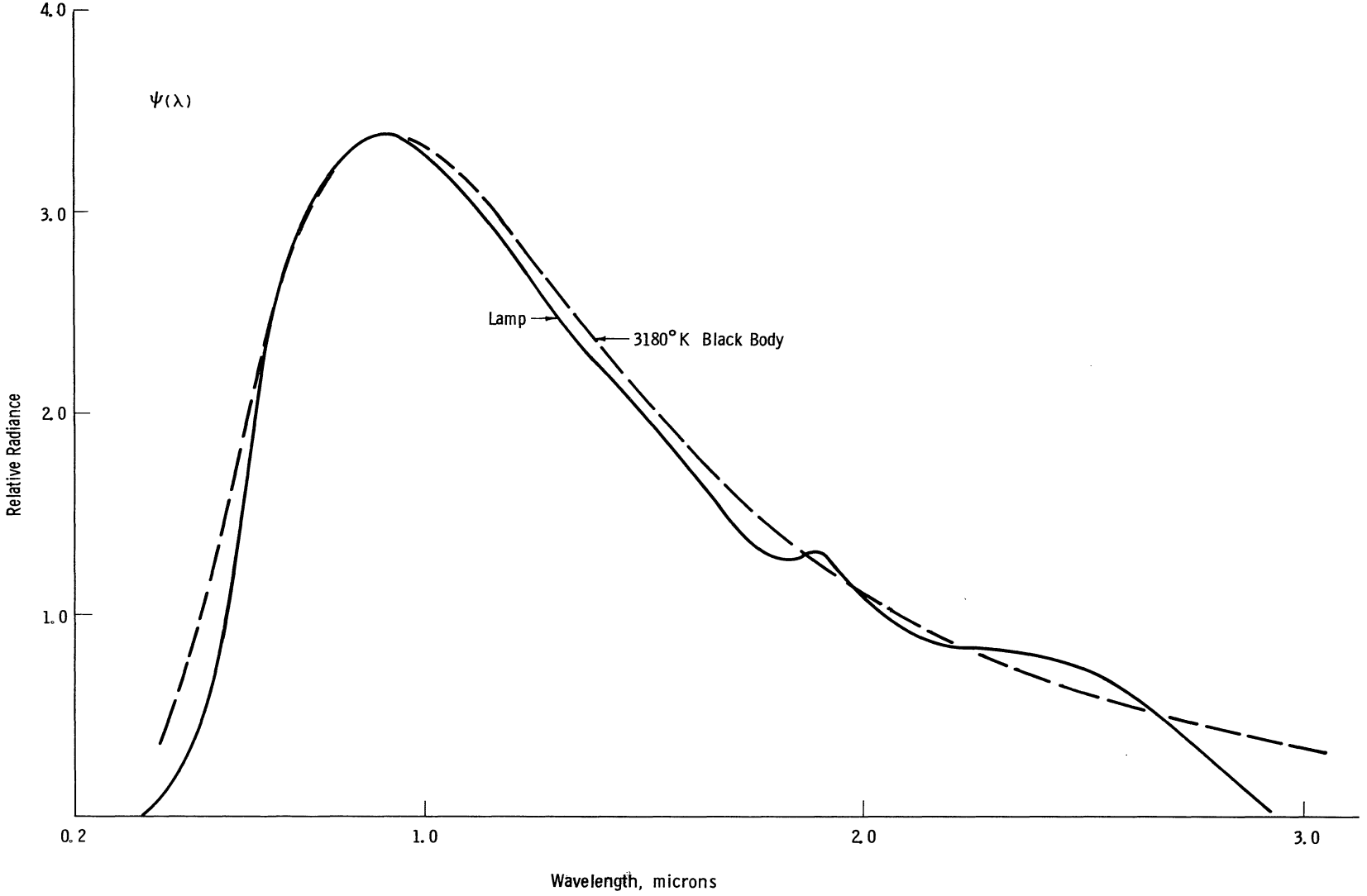

Fig. 4. Relative spectral radiance of G.E. 30A/T24/3 standard lamp No. 6271.

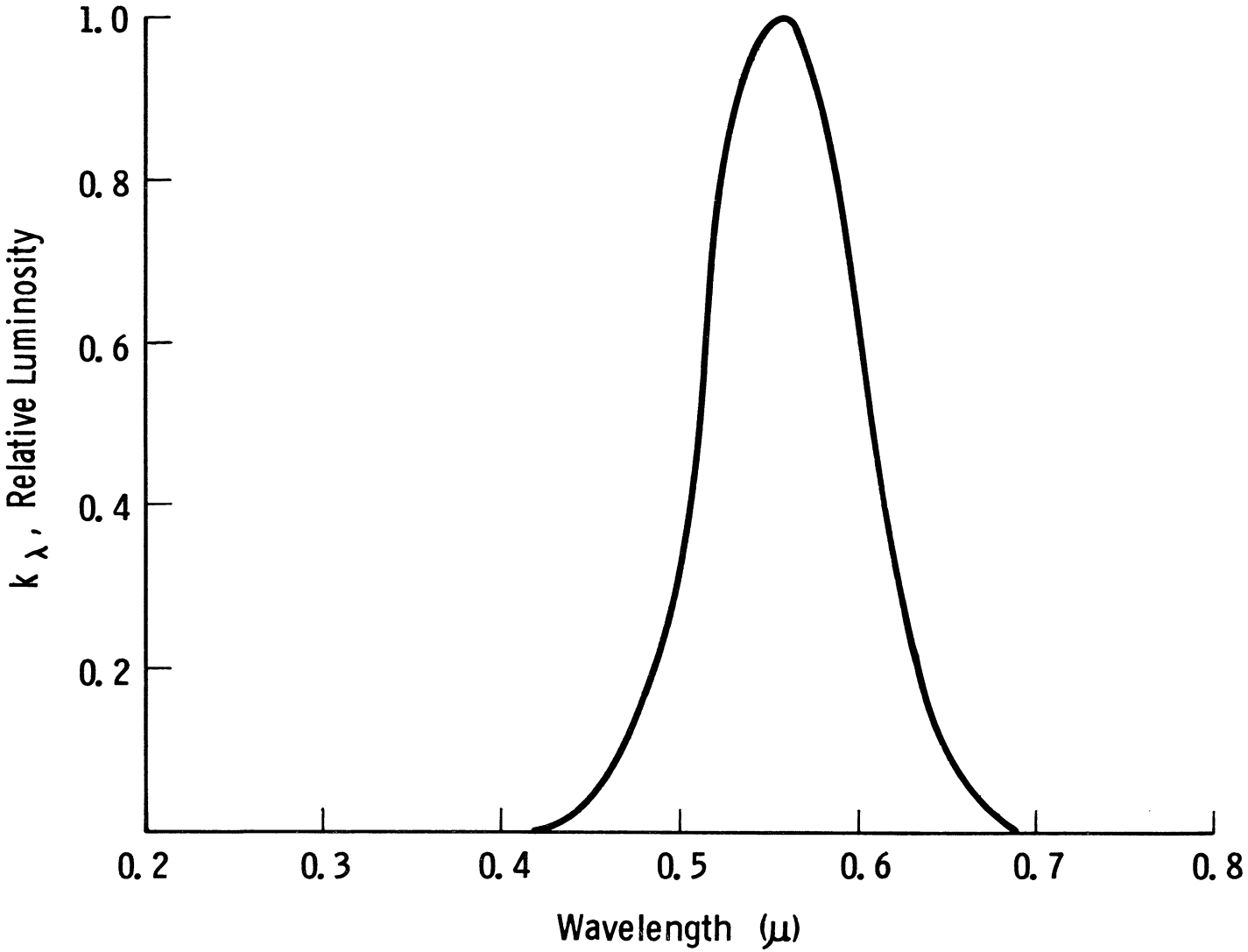

Fig. 5. Relative luminosity curve for a standard observer

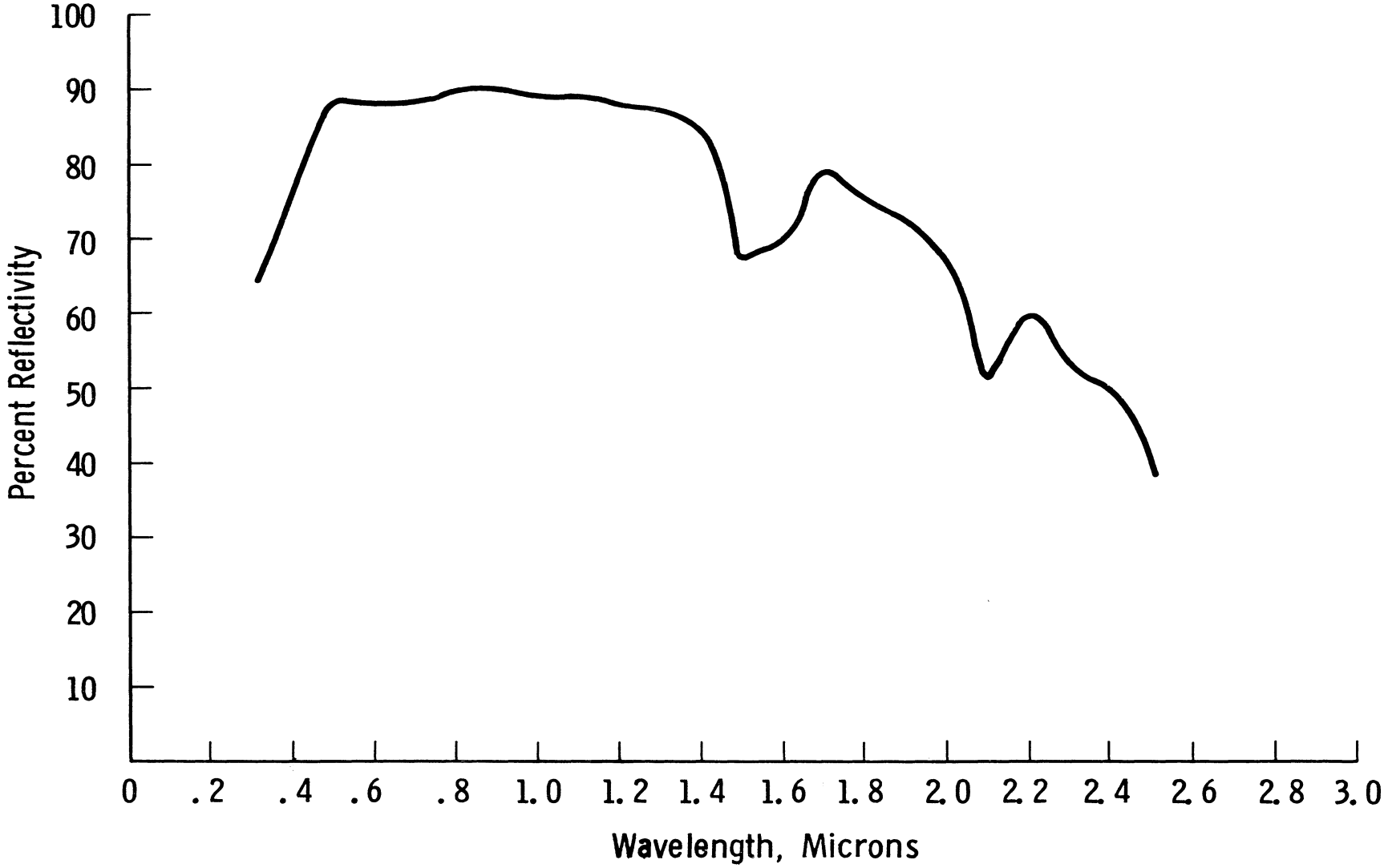

Fig. 6. Diffuse reflectivity of Kodak white paper.

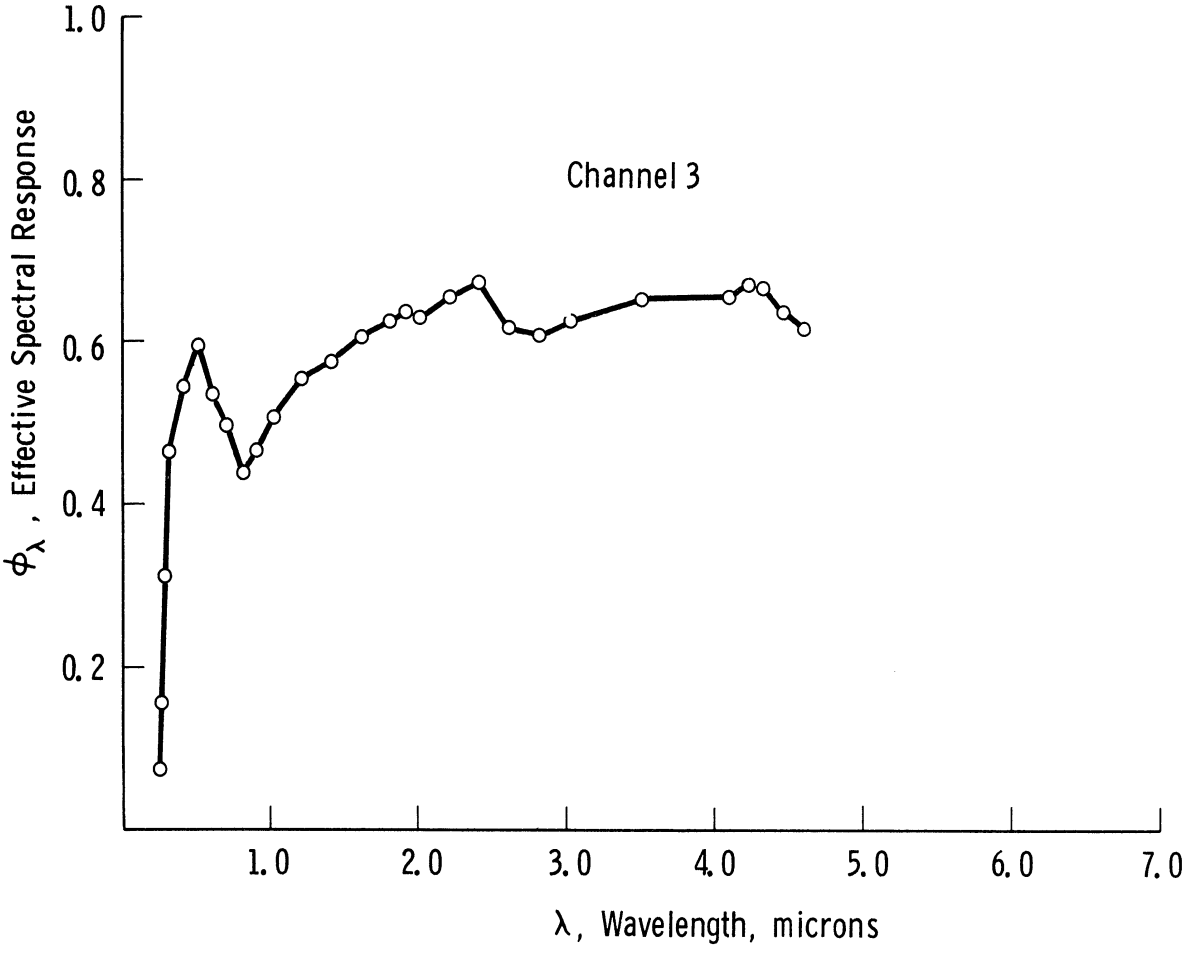

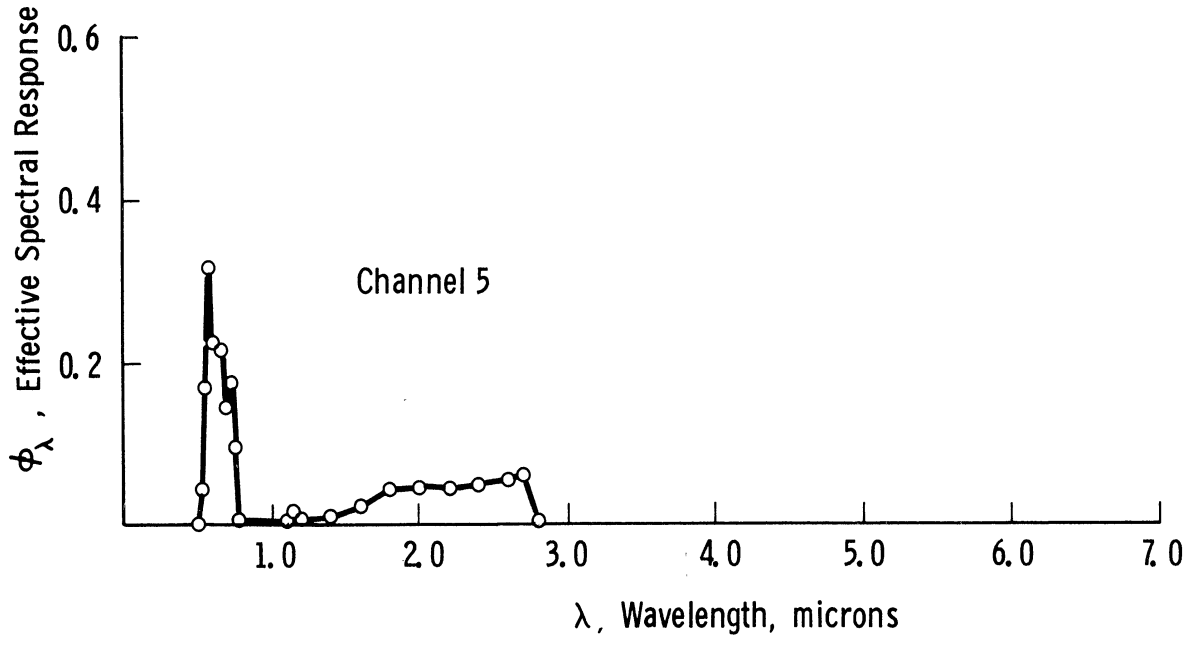

Fig. 7. Effective spectral response of channels 3 and 5 of TIROS 5-channel radiometer.

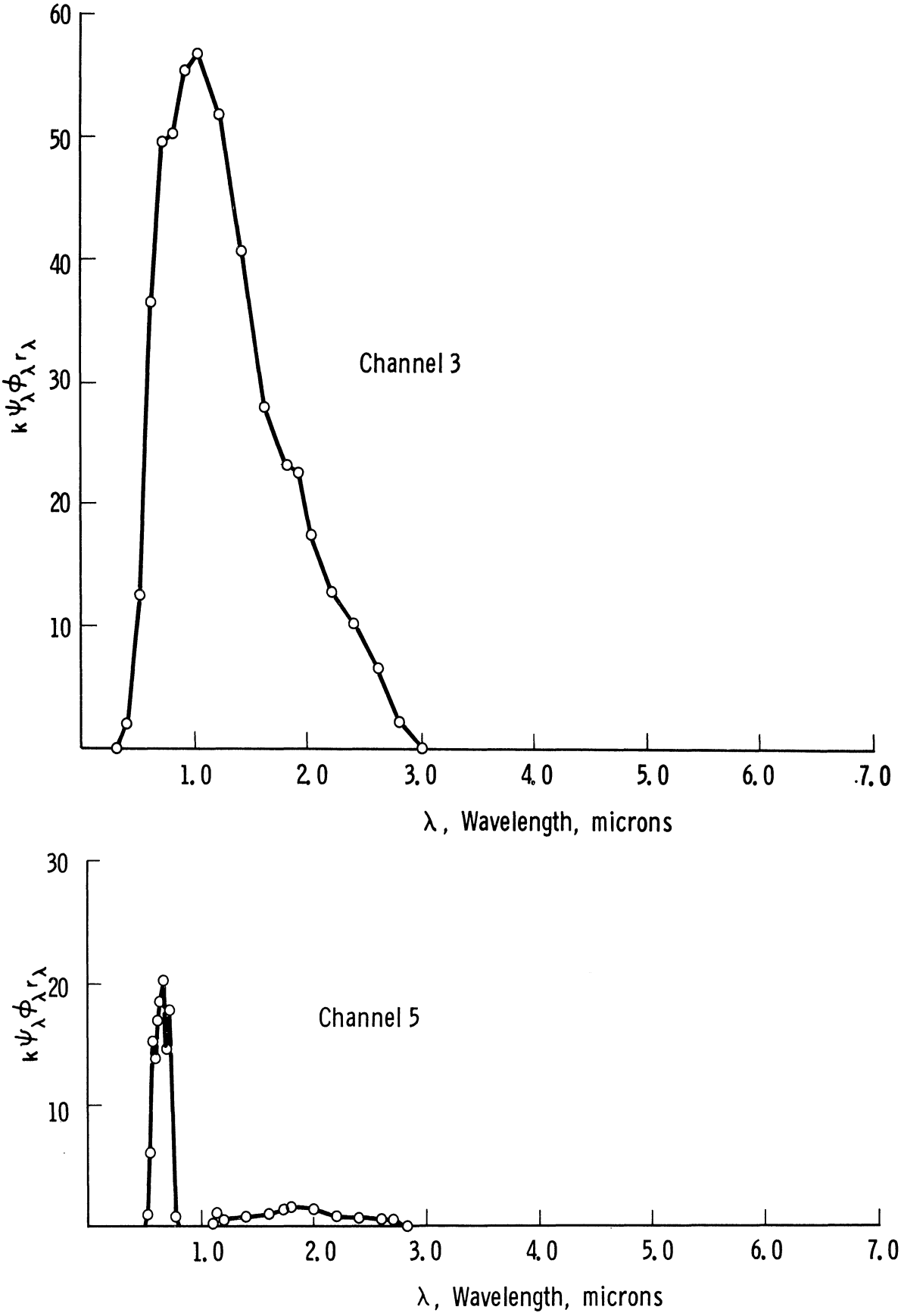

Fig. 8. White paper "effective" spectral radiant emittance, $k\psi_\lambda\phi_\lambda r_\lambda$, for TIROS 5-channel radiometer channels 3 and 5.

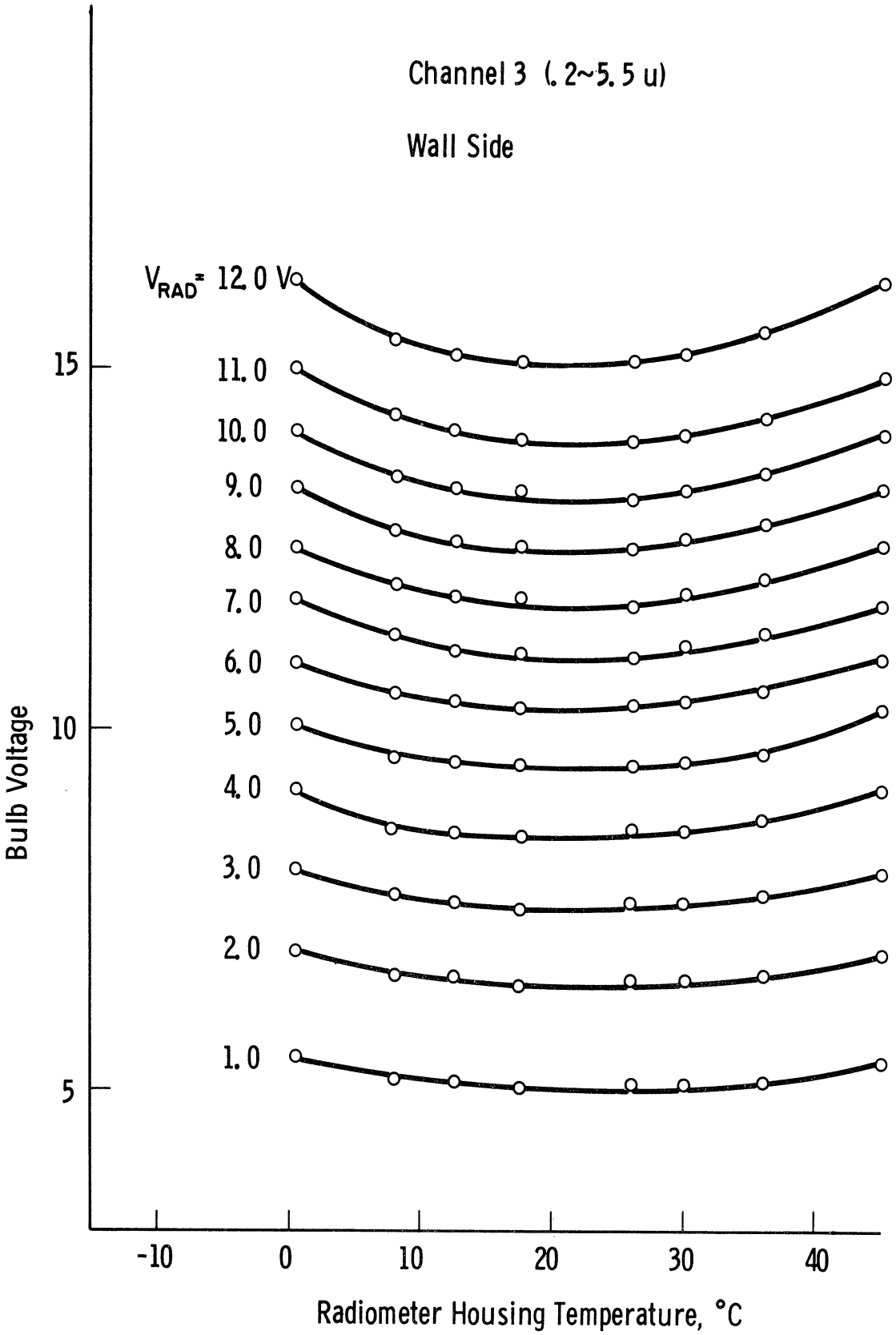

Fig. 9. Temperature dependence of calibration data for channel 3, bulb voltage vs. radiometer temperature.

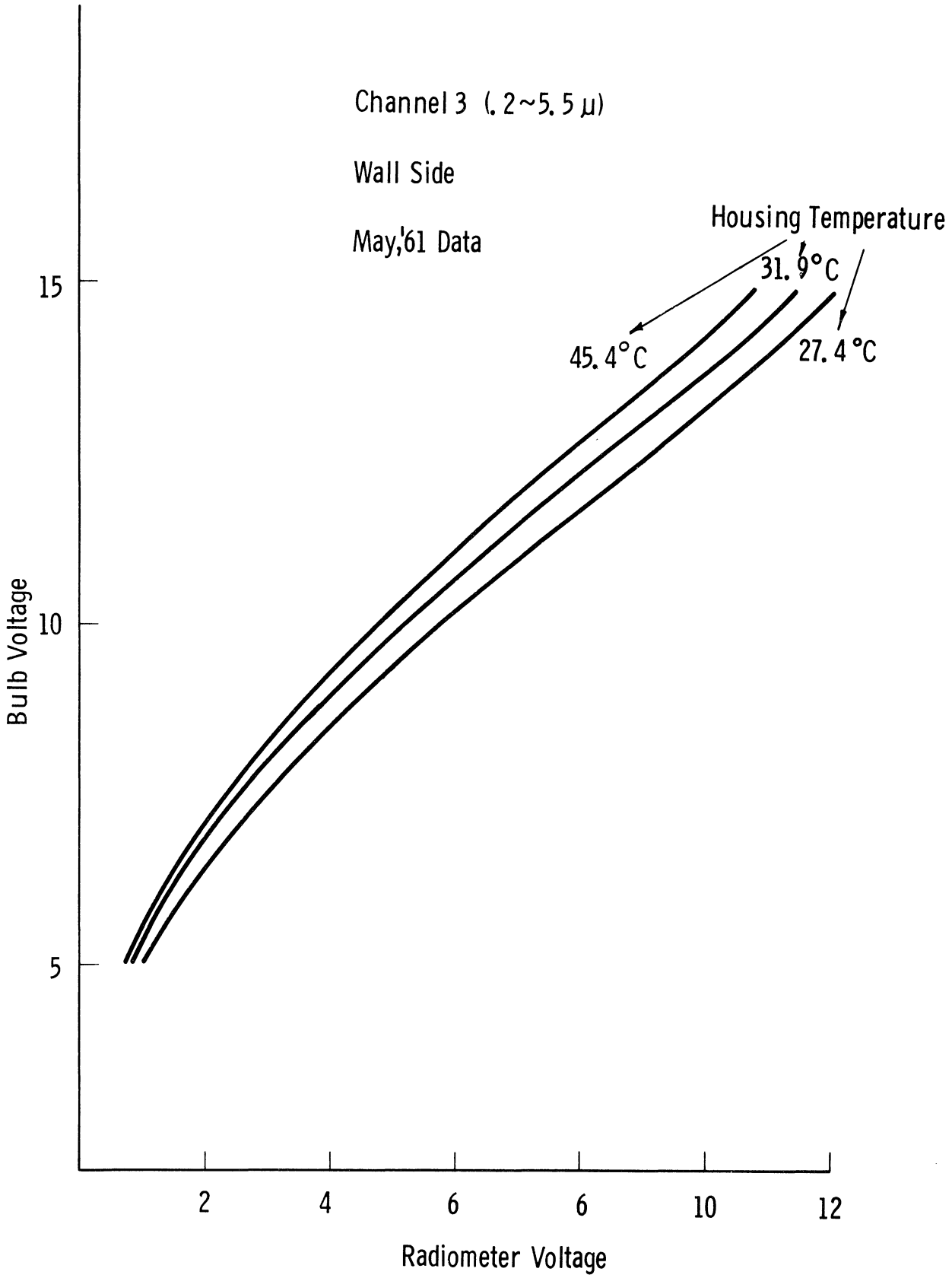

Fig. 10. Temperature dependence of calibration data for channel 3, bulb voltage vs. radiometer voltage.

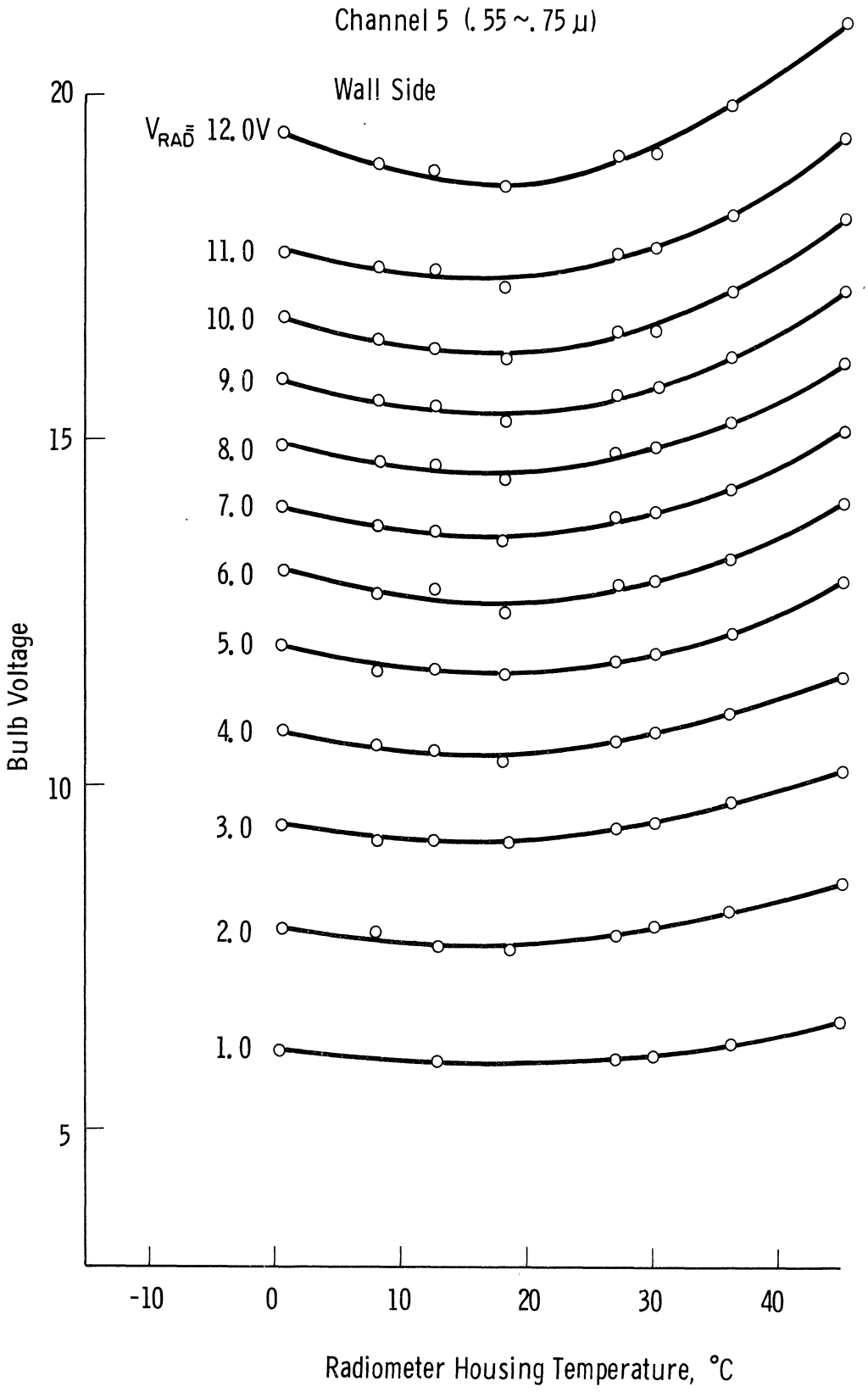

Fig. 11. Temperature dependence of calibration data for channel 5, bulb voltage vs. radiometer temperature.

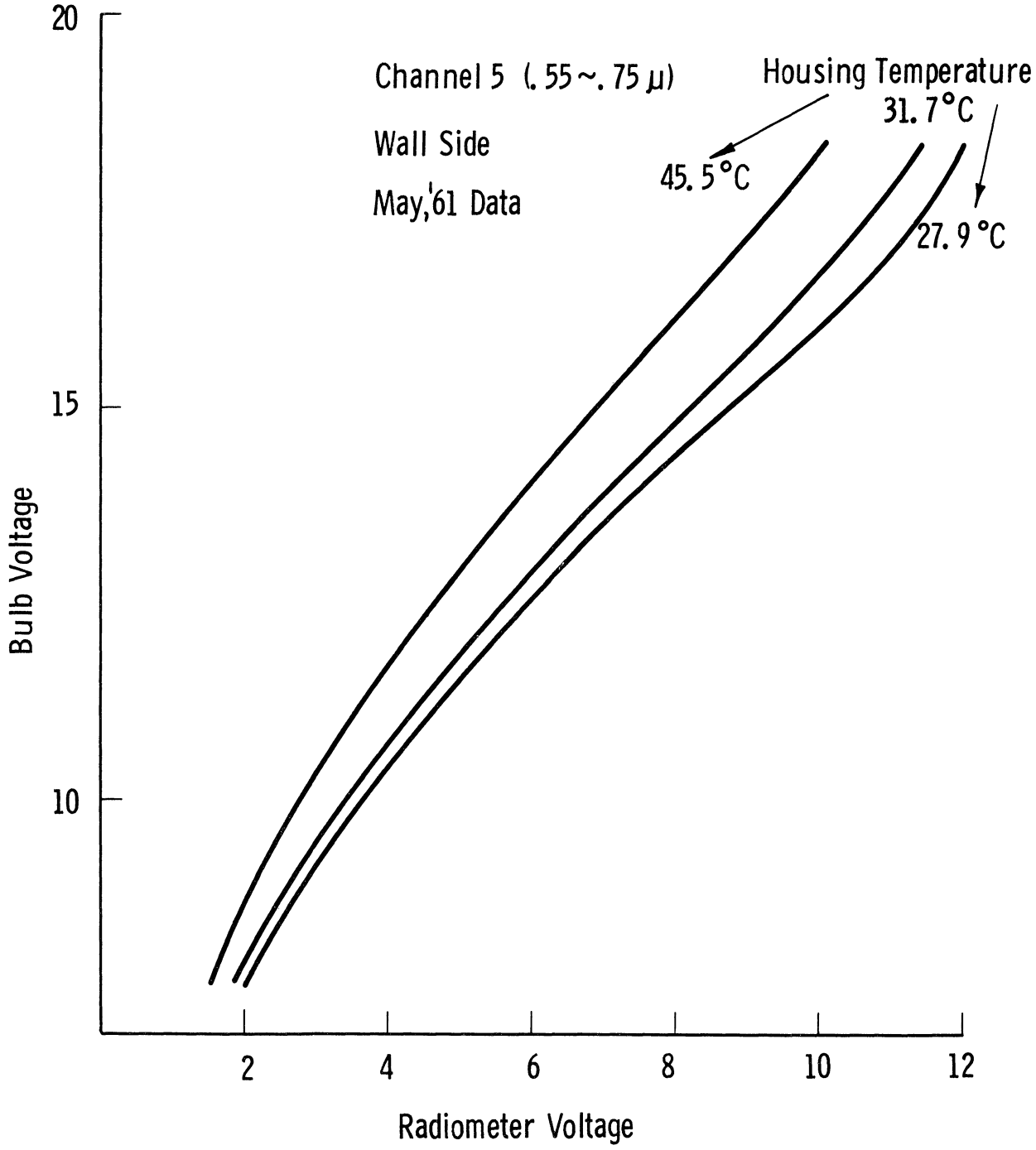

Fig. 12. Temperature dependence of calibration data for channel 5, bulb voltage vs. radiometer voltage.

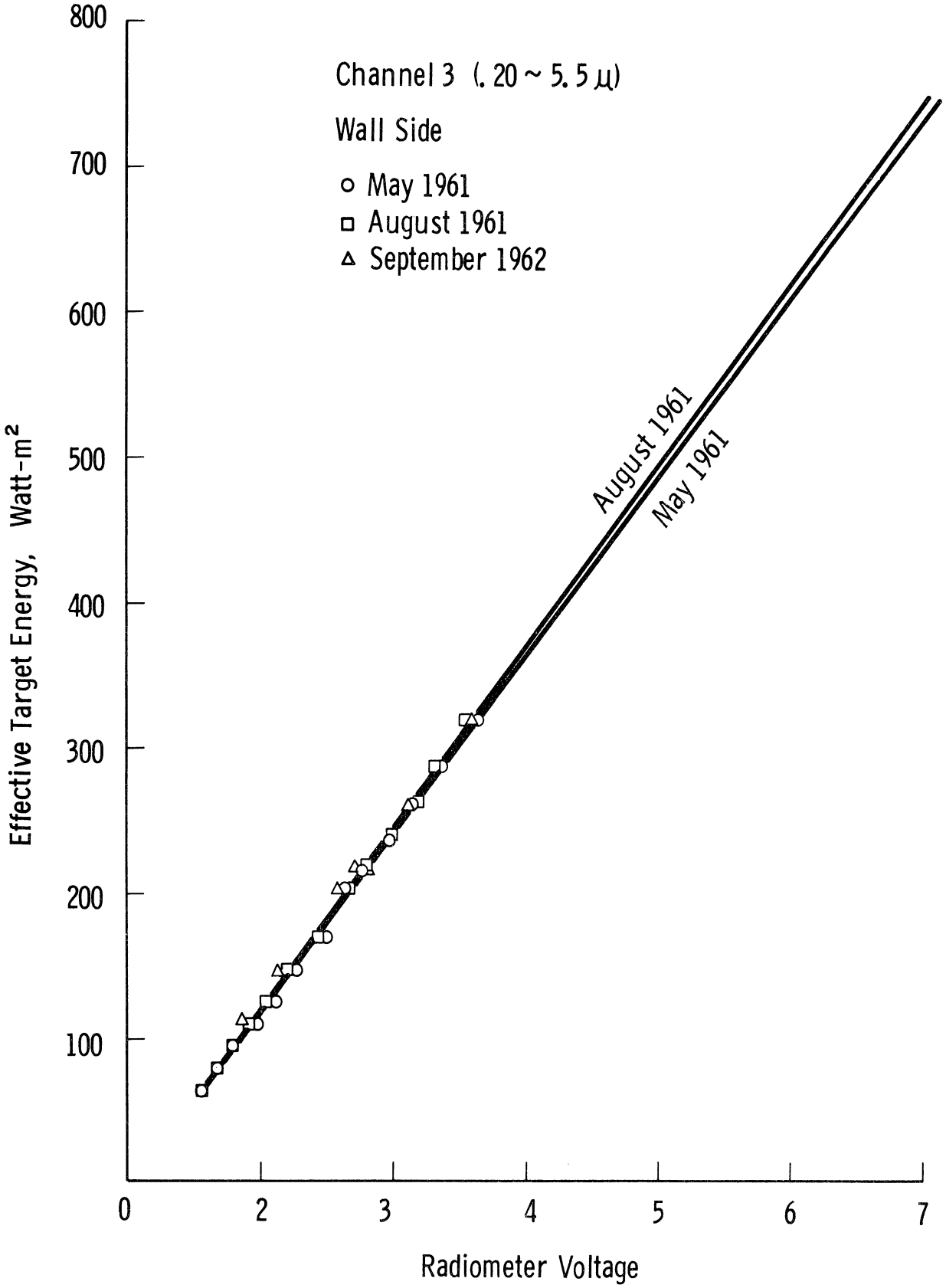

Fig. 13. Channel 3 calibration data, normalized to 30°C.

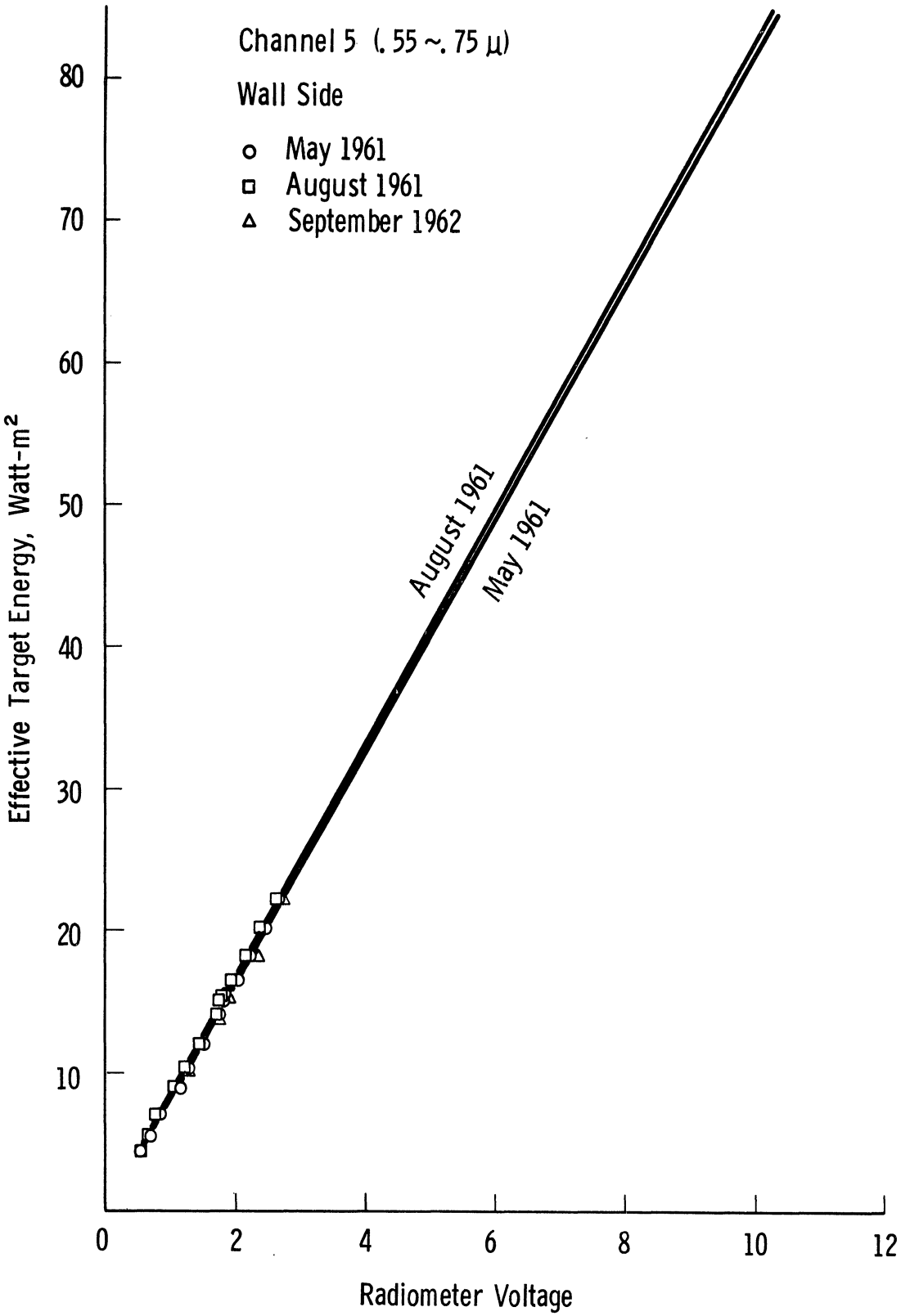

Fig. 14. Channel 5 calibration data, normalized to 31°C.

9. ACKNOWLEDGMENTS

We are deeply indebted to the Aeronomy and Meteorological Satellite Branch of NASA for financial support, for the use of their equipment in performing these calibrations, and for the kind assistance of their personnel in helping to set up the equipment and provide supplies.

10. REFERENCES

1. Astheimer, R. W., R. DeWaard and E. A. Jackson, "Infrared Radiometric Instruments on TIROS II," J. Opt. Soc. Amer., 51, pp 1386-1393, 1961.

2. Bandeen, W. R., R. A. Hanel, J. Licht, R. A. Stampfl and W. G. Stroud, "Infrared and Reflected Solar Radiation Measurements From the TIROS II Meteorological Satellite," J. Geophys. Res., 65, pp 3169-3185, 1961.

3. National Aeronautics and Space Administration and United States Weather Bureau, "TIROS II Data Users' Manual." NASA Goddard Space Flight Center, Greenbelt, Md., 15 August 1961, (Available upon request from the Aeronomy and Meteorology Division, NASA Goddard Space Flight Center).

4. Holter, M. R., S. Nudelman, G. H. Suits, W. L. Wolff, G. J. Zissis, "Fundamentals of Infrared Technology," p 54. The McMillan Co., 1962.